JPMTR-2116
DOI 10.14622/JPMTR-2116
UDC 577.1|62-4:547.4:621.798

Original scientific paper | 155
Received: 2021-12-08
Accepted: 2021-12-30

Glucomannan–xylan blend biofilms for food packaging: preparation and evaluation of filmogenic solutions and biofilms

Kholoud Al-Ajlouni, Paul D. Fleming and Alexandra Pekarovicova

Chemical and Paper Engineering,
Western Michigan University, USA

kholoudsaleh.alajlouni@wmich.edu
dan.fleming@wmich.edu
a.pekarovicova@wmich.edu

Abstract

Food packaging nowadays requires a sustainable, biodegradable, and friendly to the environment wrapping films. After cellulose, the hemicellulose in plants and grasses is the potential source for the biofilms. Konjac glucomannan is one of the hemicelluloses used to synthesize wrapping films. In this research, we conducted three sets of experiments: we formulated pure glucomannan biofilms, glucomannan–xylan blend biofilms with nano-fibrillated cellulose (NFC), and finally glucomannan–xylan blends without NFC. We studied the rheology of the filmogenic solution of the blends, before casting, and the physical and mechanical properties of the biofilms. The biofilms consisted from: glucomannan, xylan, NFC as reinforcement polymer, Surfynol 104 PA as surfactant and Sorbitol as a plasticizer. Pure glucomannan was stiff and viscous and in some cases showed a faceting phenomenon. In general, blended biofilms exhibited better properties with the presence of NFC in the formulation.

Keywords: faceting, nano-fibrillated cellulose, stretch wrapping, shear thinning, frequency sweep

1. Introduction and background

The global market for food packaging is a fast-growing one. In 2019, it was estimated as USD 303 billion and is predicted to be 503 billion in 10 years (Grand View Research, 2020). The increase of the consumer's awareness of environmentally friendly packaging and the demand for cheap, lightweight, stretchable, moisture and aroma barrier protection and printable materials, was the fuel for the continuous search for green alternatives. Wrapping films from petroleum-based plastics have the good qualities for food packaging, however, they do not exhibit biodegradability or recyclability (Honarvar, Hadian and Mashayekh, 2016). Low density polyethylene (LDPE), for example, is flexible, tough and transparent, which makes it dominating in bags or stretch film applications, but it needs 10–20 years to decompose naturally in landfill (Kunlere, Fagade and Nwadike, 2019). Bioplastics are the alternatives to plastics and they are extracted from plants, algae, shells of crustaceans and agricultural wastes. In plants, hemicellulose represents 20–30 % of the dry weight of the biomass and has 500–3 000 sugar units per polymer and dissimilar linkages (Hu, Du and Zhang, 2018). Biofilms synthesized from hemicellulose polymers are renewable, sustainable, biodegradable, and non-toxic, yet, they have proven to show semi crystallinity and hygroscopic behavior. They also allow moisture and gases to pass through them causing the food to rot. They do not stretch and elongate as plastic films, which means that their mechanical properties are poor (Hartman, 2006; Zhong, et al., 2013). One of the ways to improve the tensile strength of biofilms is blending with other polymers. Hemicelluloses have abundant number of hydroxyl groups distributed along their long backbone and frequent side chains, allowing hydrogen bond formation with other polymers; this bond is comparatively weak, but the composite film can be strong (Chen, et al., 2016). Glucomannan is a water-soluble hemicellulose found in hardwood, representing 1–4 % of the dry matter; in softwood its amount is about 20–25 % (Deshavath, Veeranki and Goud, 2019) and similarly in other plants. The content depends on the type and part of the plant from which it is extracted (Shi, et al., 2020). It is a hetero polysaccharide made up of glucose and mannose units (1 : 1.6) and its backbone consists of linked β-1,4 glyco-

sidic bonds between the sugar units (Wang, et al., 2017; Scheller and Ulvskov, 2010). Glucomannan from the tuber of konjac plant is an edible hemicellulose, viscous, dissolves easily in water and has high molecular weight. To overcome poor mechanical and barrier properties of pure glucomannan films, xylan and nano-fibrillated cellulose (NFC) have been blended with it. Xylan from corncobs makes up to 40 % of the dry matter, is a branched hetero polysaccharide whose backbone is composed of β-1,4-D-xylopyranose units with different side chains (Sasmitaloka, et al., 2019). The chemical structures of glucomannan and xylan are shown in Figure 1.

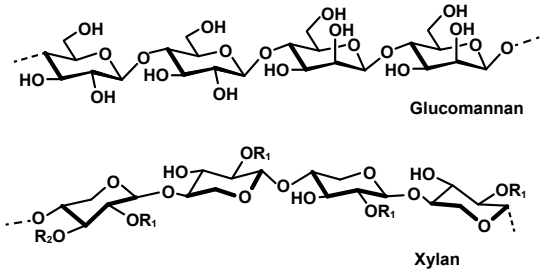

Figure 1: Chemical structure of glucomannan and xylan hemicelluloses (adapted from Nechita and Roman, 2020)

Konjac glucomannan films for food packaging improved its oxygen barrier property by using sorbitol as an external plasticizer; enhanced tensile strength by blending with NFC (Ma, Pekarovicova and Fleming, 2018), starch (Yoshimura, Takaya and Nishinari, 1998), cellulose (Kalia, et al., 2011), chitosan (Wu, et al., 2019) and others. Xylan-based packaging films suffer from poor mechanical strength, brittleness, due to strong hydrogen bonding, and moisture sensitivity. Its performance is also reinforced by cellulose, micro and nanofibrils, plasticizer and biopolymers (Zhong, et al., 2013).

Rheology is important for flow of the filmogenic or film-forming solutions of the polymers during production, the uniformity and thickness of the produced films and spreading of the ink over the films during printing (Chakravartula, et al., 2019). A rheological study of the polymers was made since all biopolymers exhibit viscoelastic behavior, that is, their viscosity decreases when the applied shear rate is increased (Lopez and Richtering, 2021; Picout and Ross-Murphy, 2003). The gel point of the film-forming solutions was determined by storage and loss moduli, G' and G'', respectively. For a polymer, if $G' < G''$ then the filmogenic solution is viscous and behaves like a liquid, else it is elastic and acts as a soft solid or gel (Morrison, 2001). The viscosity of the filmogenic solution of the biopolymers is reduced by increasing the applied shear rate, because the bonds were broken and the particles present in the aqueous suspension are ruined by shear (Triantafillopoulos, 1988). In a previous work, we used konjac glucomannan to make packaging films, but we confronted a phase transformation of the polymer droplets and freezing of the surfactant at the glucomannan–water interface. This phenomenon is called faceting, and triggered the deformation of glucomannan spherical droplets into distorted polygons and long thin fibers. Uncontrolled slow cooling with the presence of the surfactant was the reason behind faceting. The 3D structure of the frozen surfactant made the produced films non-transparent, weak and gas permeable (Al Ajlouni, Fleming and Pekarovicova, 2021). In this work, the glucomannan–xylan biofilms studied were divided into three sets: pure glucomannan, glucomannan–xylan blends reinforced with NFC, and glucomannan–xylan blends without NFC. The aim is to see the effect of xylan and NFC on the properties of blend films all together.

2. Experimental

In the first sets of the studies (Al Ajlouni, Fleming and Pekarovicova, 2021), a shape deformation of pure glucomannan droplets emulsion in the surfactant solution showed up, and resulted in hard, rough and polygon surface, which was revealed after drying and did not show upon casting. The surfactant lowered the surface tension of the glucomannan drops at the interface with water and made them lose their spherical shape into polygons; this phenomenon is known as faceting. The authors studied the effect of the surfactant of faceting of the biofilms. The concentrations were 0.05–0.4 g of the surfactant in 100 ml of DI water. The films gained thickness but lost some of their optical, physical and mechanical properties.

2.1 Materials

Xylan from corncob, Biosynth Carbosynth company, molecular weight: 300–900 Da; glucomannan from konjac, NOW Food Company, molecular weight: $(0.2–2) \times 10^6$ Da (Now Foods, n.d.); Surfynol 104 PA, Air Products and Chemical Inc.; Sorbitol, Alfa Aesar, molecular weight: 182.17 Da, and deionized (DI) water from WMU. The components of each film are given in Table 1. The name of the films represents the amount of glucomannan mass in the film formulation, for example, Gluc90 means 0.9 g glucomannan with 0.1 g xylan dissolved in 100 ml of DI water. The other ingredients are kept constant: Surfynol 104 PA, NFC and Sorbitol.

2.2 Glucomannan–xylan biofilms synthesis

Glucomannan was dissolved in 100 ml of DI water at room temperature and then transferred into a water bath at 40 °C, where the solution was mixed for 15 minutes by a rotary mixer. The surfactant, Surfynol 104 PA, was added to the solution and mixed for 3 minutes followed by xylan, which was mixed for 5 minutes.

Table 1: Glucomannan and glucomannan–xylan films showing NFC contributions (in 100 ml DI water)

	Film's name	Glucomannan [g]	Surfynol 104 PA [g]	Xylan [g]	NFC [g]	Sorbitol [g]
Pure	Gluc100	1.0	0.1	0	0.1	0.2
Without NFC	Gluc90	0.9	0.1	0.1	0	0.2
	Gluc80	0.8	0.1	0.2	0	0.2
	Gluc70	0.7	0.1	0.3	0	0.2
	Gluc60	0.6	0.1	0.4	0	0.2
	Gluc50	0.5	0.1	0.5	0	0.2
	Gluc40	0.4	0.1	0.6	0	0.2
With NFC	Gluc90	0.9	0.1	0.1	0.1	0.2
	Gluc80	0.8	0.1	0.2	0.1	0.2
	Gluc70	0.7	0.1	0.3	0.1	0.2
	Gluc60	0.6	0.1	0.4	0.1	0.2
	Gluc50	0.5	0.1	0.5	0.1	0.2
	Gluc40	0.4	0.1	0.6	0.1	0.2

NFC was mixed for 5 minutes more and finally Sorbitol for 3 extra minutes. In pure glucomannan experiments, xylan was not added. For density, viscosity, rheology, contact angle and surface energy tests, a 5–10 ml sample of the film-forming solution was collected and tested. The rest of the film-forming solution was casted in a Petri dish and dried at 60 °C and 35 % RH. After drying, the film was peeled off and stored in the testing lab for conditioning before testing based on TAPPI's conditions: 50 % RH, 23 °C for 24 hours. For film characterization, some tests were accomplished and compared with the control sample, LDPE film.

2.3 Filmogenic solutions' tests

2.3.1 Density

Density is measured by a Gardco pycnometer, which has an exact volume of 8.32 ml at 20 °C. The mass of the filmogenic solution is calculated by the difference of the masses of the cup, with and without the solution, and the density is calculated in g/cm^3.

2.3.2 Viscosity and rheology

An Anton Paar rheometer was used and a rheogram of the apparent viscosity vs. shear rate was produced; the shear rate range was 0.1–1000 s^{-1}. The value of the storage and loss shear moduli under frequency sweep test were determined and plotted, and the point where the film-forming solution turns into gel was detected.

2.3.3 Surface tension of filmogenic liquids before drying

A FTA200 instrument was used for contact angle and surface tension measurements by recording a video of drops of a fluid falling over a substrate by a controlled needle pump and a camera capturing 300 images per run.

2.4 Non-destructive tests of the biofilms

Non-destructive tests are the tests that keep the sample as it is before testing; these were done first. Examples of non-destructive tests are: measurement of thickness, roughness, air permeability, opacity, transparency and other properties.

2.4.1 Thickness of the glucomannan–xylan biofilms

After conditioning the biofilms, the thickness or caliper was measured by Technidyne Profile Plus machine. Its accuracy is ± 0.508 mm. The thickness of the films depends on the type of mold used in casting the filmogenic solution, and the drying conditions. Once the solution was poured into a Petri dish, it was levelled and started cooling. Air flow inside the Caron environmental chamber was not circulated evenly on the surface, which caused little variations in the thickness of the biofilms between the center and at the rim. Thickness influences roughness, transparency, permeability, tensile strength and % elongation of the films.

2.4.2 Transmittance and transparency

Transmittance is the ratio between visible light transmitted through the film to that falling on the surface, expressed as a fraction *T* and governed by Beer's law (Ingle and Crouch, 1988). Transparency is usually characterized by light transmittance, type of polymer crystallinity and types of additives used. Crystalline or semi-crystalline polymers, LDPE for instance, are opaque because there are amorphous and crystalline regions, which make transmission different.

A Spectroscan auto scanner measures the transmission of visible light, in the range of 280–600 nm, passing through the biofilm according to ISO 13468–1 (International Organization for Standardization, 2019).

Transparency is defined as:

$$\text{transparency} = -\log(\text{transmittance/thickness}) \quad [1]$$

Equation [1] depends on the unit of length used to measure the thickness. If the thickness is measured in mm, the transparency is given in terms of the transmittance of 1 mm thick sample. This is based on how transparency scales with thickness according to the Beer–Lambert law (Ingle and Crouch, 1988). If the amount of light transmitted through the biofilm is high, the higher the transparency will be.

2.4.3 Air permeability

Parker Print Surf instrument measures the "PPS porosity" of the biofilms in ml/min, and air permeability coefficient K is calculated according to TAPPI T 555 (Technical Association of the Pulp and Paper Industry, 2010). Air permeability (PPS porosity) means the ability of the films to let air pass through as a result of air pressure difference on both sides for 5 seconds and it has the units of (mm^2 for permeability, or ml/min for PPS porosity) (IGT team, 2021). Darcy's equation describes the fluid flow through any porous material, where the flow rate of the fluid is a function of the pressure drop across the sample, area of flow and viscosity of the fluid and defines the permeability coefficient K (m^2). Pal, Joyce and Fleming (2006) proposed a method to calculate the permeability coefficient based on PPS porosity values in ml/min at 1 000 kPa air pressure with viscosity of air at 23 °C of 1.8×10^{-5} Pa·s, area of 10 cm^2 and air pressure drop of 6.17 kPa between the two sides. The relation becomes:

$$K = 0.048838 \times Q \times L \quad [2]$$

where K is given in μm^2, Q is air flow rate in ml/min and L is the thickness of the film in m, the number 0.048838 contains the constant values, such as viscosity of air and the area of the sample (Pal, Joyce and Fleming, 2006). This property is essential for packaging biofilms to protect food from getting spoiled or altered by chemical reactions with air or moisture.

2.5 Destructive tests of the biofilms

The destructive tests are the tests that deform or damage the specimen upon testing and it is done to identify physical and chemical properties of the material. One example is tensile test.

2.5.1 Tensile strength and % elongation

The ability of the packaging films to stretch and ensure a good seal is expressed in terms of tensile strength and % elongation of the films. High tensile strength keeps the products secured and sealed during shipping.

An Instron instrument was used to test the tensile and elongation of the films. The samples were cut as a strip of 100 mm × 15 mm, gripped in Instron clamps and pulled apart under a 500 N load and with a speed of 2.5 cm/min until it breaks. The software accompanied with the machine reports the values and plots the results of tensile strength at break and % elongation at break or strain among other properties.

3. Results and discussion

3.1 Faceting of glucomannan polymer

In Figure 2, the surface of the deformed biofilms after drying (at 50 °C and 11.4 % RH) shows clear polygon shapes and solid boundaries. The best concentration of Surfynol 104A used in the experiments is 0.1 g in 100 ml DI water. Upon testing, the films gained thickness but lost some of their optical, physical and mechanical properties.

3.2 Results of filmogenic solutions' tests

Characterization of the filmogenic solutions started with the density. The density of the all the samples was measured by Gardco pycnometer at 20 °C and rounded to three significant figures, so the density was 1 g/cm^3 or 1 000 kg/m^3 for all samples. All results, including the values for xylan, are listed in Table 2.

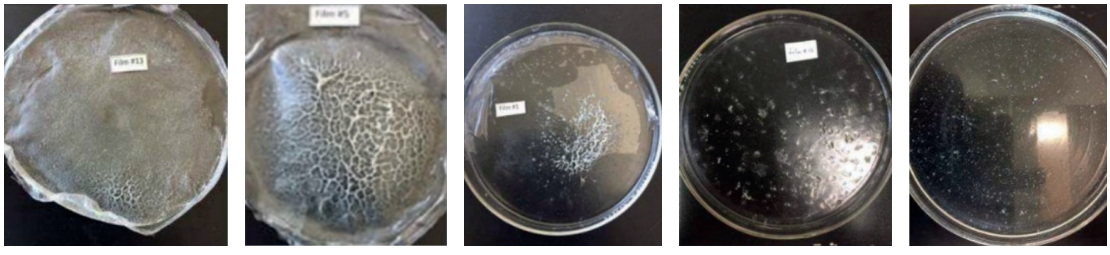

a) *b)* *c)* *d)* *e)*

Figure 2: Faceted glucomannan biofilms (a) to (d) and a successful one (e) (adapted fromAl Ajlouni, Fleming and Pekarovicova, 2021)

Table 2: Some properties of the filmogenic of glucomannan, glucomannan–xylan and xylan solutions

	Filmogenic film	Density [g/cm³]	Apparent viscosity at 100 s^{-1} [mPa·s]	Contact angle [Angle]	Surface tension [mN/m]
Pure	Gluc100	1.0	1 333	57	38
Without NFC	Gluc90	1.0	1 169	54	45
	Gluc80	1.0	767	55	46
	Gluc70	1.0	611	62	43
	Gluc60	1.0	384	56	41
	Gluc50	1.0	263	57	41
	Gluc40	1.0	179	52	42
With NFC	Gluc90	1.0	1 117	68	45
	Gluc80	1.0	773	62	46
	Gluc70	1.0	576	56	45
	Gluc60	1.0	410	51	44
	Gluc50	1.0	238	44	42
	Gluc40	1.0	72	42	42
	Xylan	0.9	68	23	43

3.2.1 Viscosity

The apparent viscosity in Table 2 shows that the pure glucomannan film is the most viscous one having 1333 mPa·s at 100 s^{-1}. The viscosities of the film-forming solutions without the presence of NFC were higher than the solutions had when NFC was added, with exception for Gluc80 and Gluc60. For example, Gluc90 filmogenic solution viscosity without NFC was lowered from 1167 to 1117 mPa·s. Similarly, increasing the concentration of the glucomannan made the film-forming solutions more viscous, due to the highly viscous nature of glucomannan and higher molecular weight as illustrated in Figure 3.

3.2.2 Rheology

The Anton Paar Rheometer with a parallel plate measuring system used a frequency sweep test to measure the loss G'' and storage G' moduli, in the range of 0.01 to 100 rad s^{-1} at 25 °C and under shear strain of 5 %. Figure 4 demonstrates the viscoelastic behavior of pure glucomannan filmogenic solution.

Reinforced pure glucomannan turned into a gel at 63 rad/s, whereas the non-reinforced became a gel earlier at 3.6 rad/s. This implies that the internal friction between the molecules and particles is higher due to NFC addition to the polymer matrix. The same arguments can be said about glucomannan–xylan filmogenic solutions illustrated in Figure A1 in Appendix. A comparison of the rheological behavior of each filmogenic solution is presented between that reinforced with NFC (Figure A1a) and that without NFC. A summary of the loss and storage moduli is listed in Table 3, evaluated at 100 rad/s.

The glucomannan–xylan filmogenic solutions with NFC were gelling slower than the same solutions without NFC, i.e. $G' > G''$, which means that NFC hindered the gelation process. Also, the storage modulus was greater than the loss modulus $G' > G''$ for higher gluco-

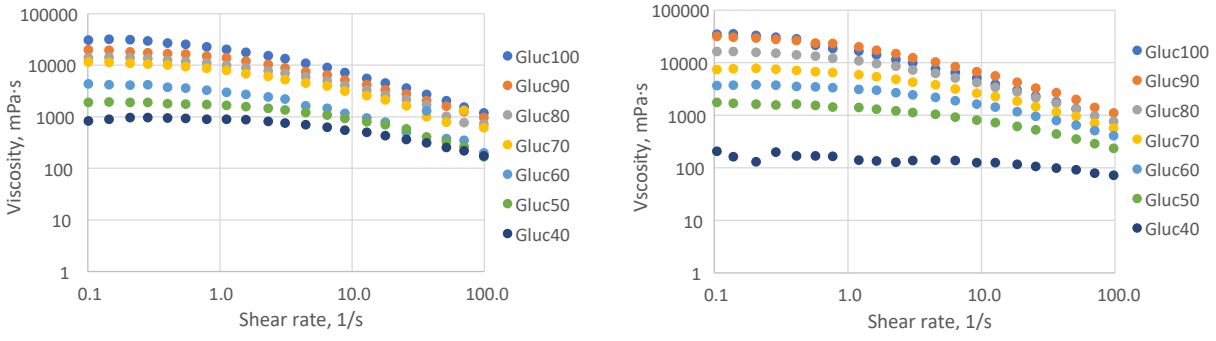

a) *b)*

Figure 3: Viscosity of filmogenic solutions of glucomannan and glucomannan–xylan, without NFC (a) and reinforced with NFC (b)

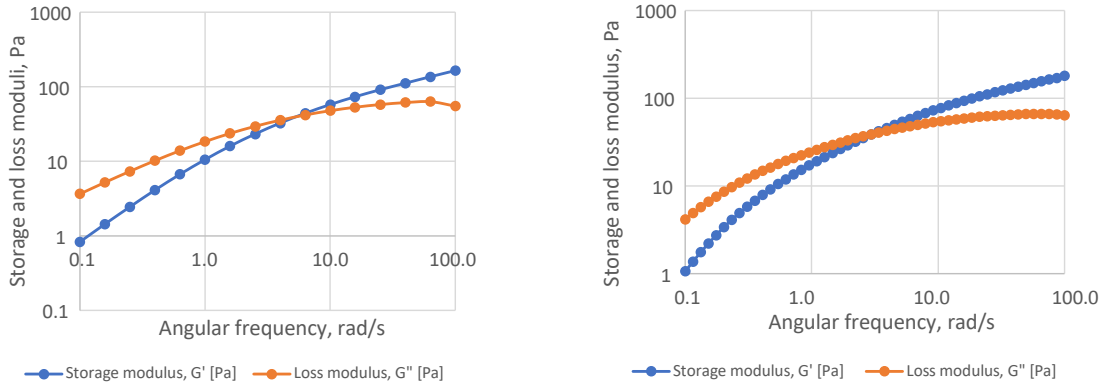

a) *b)*

Figure 4: Frequency sweep for pure glucomannan filmogenic solutions reinforced with NFC (a) and without NFC (b)

mannan concentrations (Gluc100–Gluc70) and Gluc40, but Gluc60 and Gluc50 without NFC had $G' < G''$, which indicated that both started gelation earlier than the other samples.

Table 3: Storage and loss moduli of glucomannan and glucomannan-xylan filmogenic solutions at 100 rad/s

	Filmogenic film	Storage modulus, G' [Pa]	Loss modulus, G'' [Pa]
Pure	Gluc100	179	64
Without NFC	Gluc90	174	76
	Gluc80	139	21
	Gluc70	30	18
	Gluc60	21	25
	Gluc50	5	12
	Gluc40	15	8
With NFC	Gluc100	165	55
	Gluc90	112	70
	Gluc80	129	21
	Gluc70	62	36
	Gluc60	20	22
	Gluc50	8	3
	Gluc40	5	2

3.2.3 Surface tensions and contact angles

Figure 5 shows a demonstration of the contact angle and a pendant drop of glucomannan over glass measured by FTA200. The blends of glucomannan–xylan were tested for the effect of the NFC on the formulation of the biofilms. The NFC revealed a direct increase in the value of the contact angles of the filmogenic solutions.

Pure glucomannan filmogenic solution possessed a 57° contact angle (rounded on two digits), which implies that wettability of the solution onto the surface of glass is low. The contact angle of all solutions exceeded 40°, however, the average of the solutions' contact angles without NFC was higher than that with NFC, 56° and 54°, respectively. The values of the contact angles of the blends of glucomannan–xylan were less than pure glucomannan, which may give an indication that xylan reduced the contact angle and increased the wettability of the blends. Xylan has a small contact angle of 23° and a surface tension 43 mN/m, therefore, when the amount of xylan is increased, it contributes in reducing the contact angles of the overall solutions, as shown in Figure 6.

a) *b)*

Figure 5: Contact angle and surface tension of a drop over a substrate when surface tensions between each two phases are in equilibrium (Makkonen, 2016) (a); and a drop of pure glucomannan filmogenic solution over glass, with contact angle 57.29° for 0.1 g surfactant in pure glucomannan (Al Ajlouni, Fleming and Pekarovicova, 2021) (b)

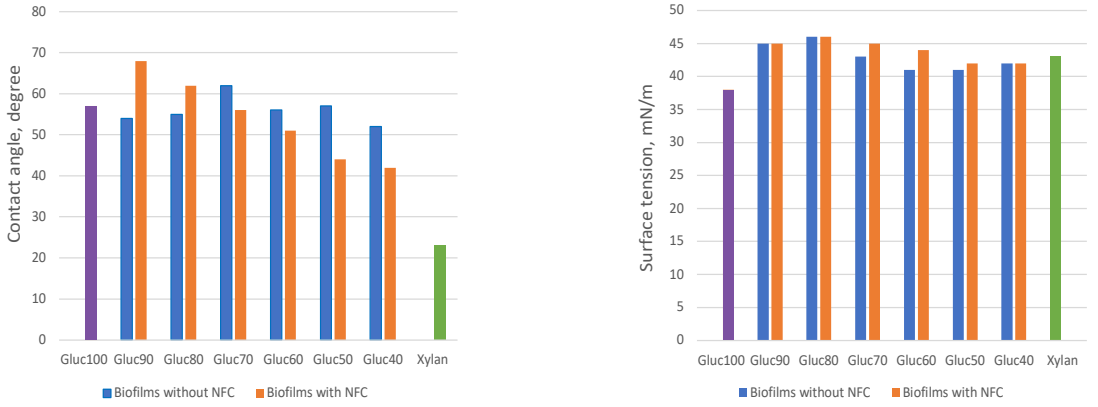

a) *b)*

Figure 6: The contact angles (a), and surface tensions (b) of filmogenic solutions of glucomannan, glucomannan–xylan biofilms, and xylan

3.3 Results of non-destructive testing of glucomannan–xylan biofilms

The non-destructive tests are illustrated in Table 4 and the graphs are shown in Figure 7 for all samples compared with LDPE film.

3.3.1 Thickness of glucomannan–xylan biofilms

The thickness of the biofilms was measured and the average of 5 readings was recorded as illustrated in Table 4 and shown in Figure 7. The changes in the thickness due to air flow on the surfaces appeared during the drying process; the areas close to the edges of the Petri dish were thinner than the middle, so leveling and thickness were not the same. The addition of NFC increased the caliper of the biofilms, maybe because it made extra bonding between the components of the biofilms and made it tighter and thicker. Only Gluc80 deviated from the trend, there was 7.6 µm difference between the two cases of NFC presence or not.

3.3.2 Transmittance and transparency

As given in Table 4, LDPE has a highest transmittance of 96 %, which is obvious since it is semi-crystalline. All the films showed an average > 71 % transmittance; the films Gluc100 to Gluc50 have almost close % transmittance, average of 77 %, but Gluc40 deviated by almost 12 %. This may indicate that the structure of the glucomannan–xylan biofilms is semi-crystalline. We may also conclude that the glucomannan concentration enhanced the % transmittance of visible light through the polymer blend matrices.

Table 4: Results of non-destructive tests of glucomannan and glucomannan–xylan films

	Filmogenic film	Thickness [µm]	Transmittance [%]	Transparency (Eq. [1])	PPS roughness [µm]	PPS porosity [ml/min]	Air permeability coefficient (Eq. [2]) [µm²]
Pure	Gluc100	62.01	79.0	1.89	4.34	1.34	4.1×10^{-6}
Without NFC	Gluc90	76.44	80.8	1.98	5.94	1.57	5.9×10^{-6}
	Gluc80	87.60	80.1	2.04	2.13	0.71	3.0×10^{-6}
	Gluc70	96.52	78.7	2.09	0.32	0.33	1.6×10^{-6}
	Gluc60	116.58	73.3	2.20	1.64	0.11	6.3×10^{-7}
	Gluc50	140.13	70.3	2.30	0.83	0.14	9.6×10^{-7}
	Gluc40	108.15	55.2	2.29	0.61	0.36	1.9×10^{-6}
With NFC	Gluc100	71.75	87.6	1.91	6.63	0.84	2.9×10^{-6}
	Gluc90	83.78	75.4	2.05	7.33	0.59	2.4×10^{-6}
	Gluc80	80.00	68.6	2.07	5.43	0.34	1.3×10^{-6}
	Gluc70	105.91	71.3	2.17	1.36	0.18	9.3×10^{-7}
	Gluc60	150.28	66.8	2.35	2.67	0.08	5.9×10^{-7}
	Gluc50	155.18	65.5	2.37	5.94	0.90	6.8×10^{-6}
	Gluc40	134.33	53.0	2.40	1.95	0.45	3.0×10^{-6}
	LDPE	118.00	96.0	2.09	0.11	0.10	8.8×10^{-8}

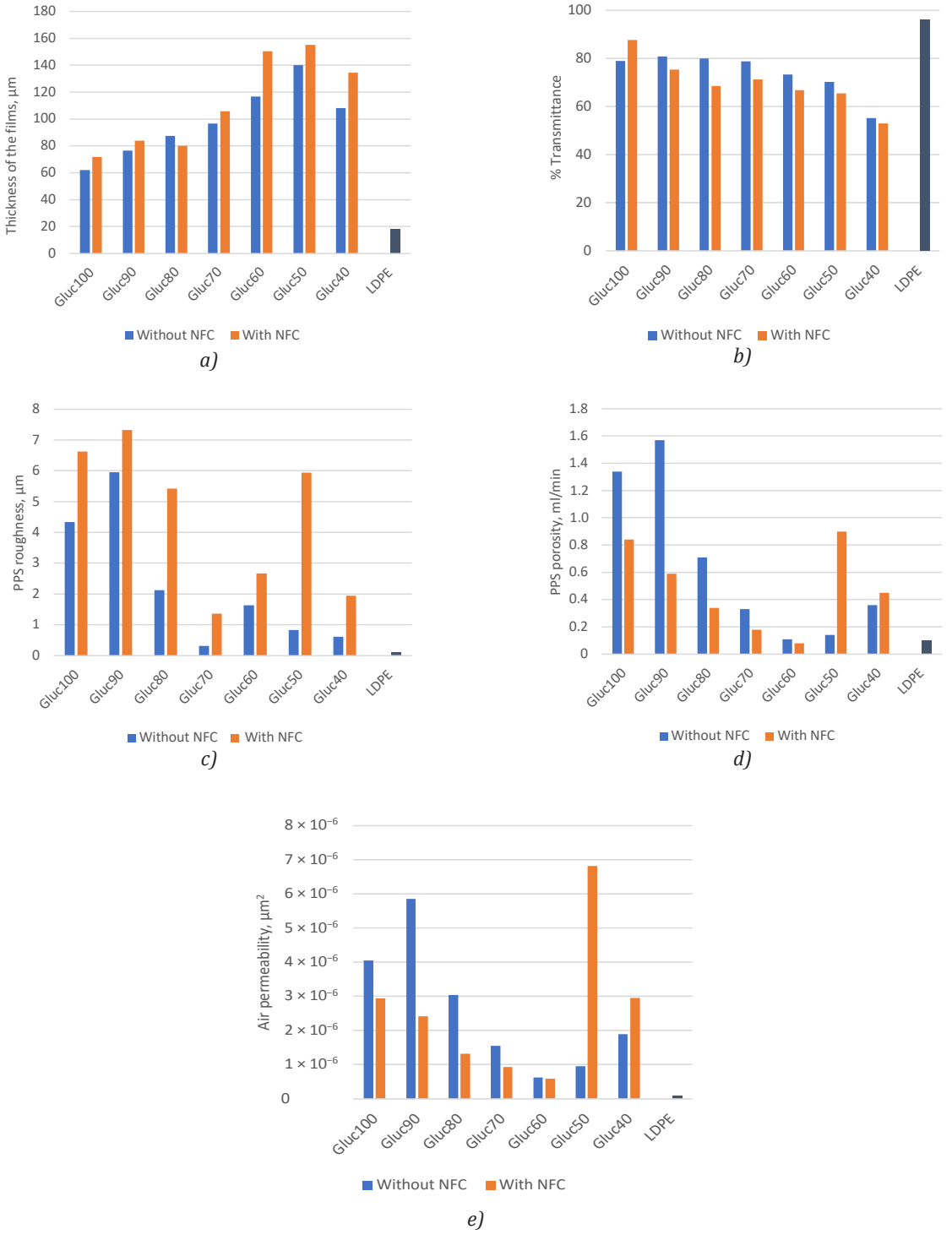

Figure 7: Non-destructive tests of glucomannan, glucomannan–xylan biofilms, reinforced with NFC and without NFC, compared with LDPE films: thickness (a), transmittance (b), PPS roughness (c), PPS porosity (d), and air permeability (e)

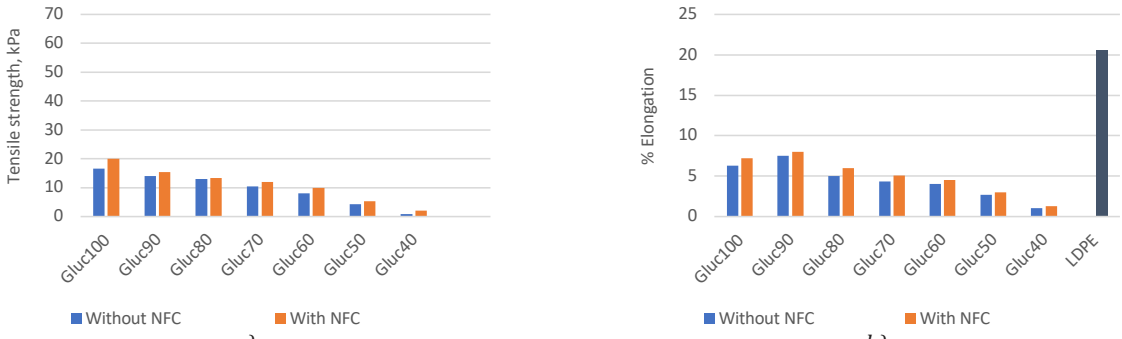

a) *b)*

Figure 8: Tensile strength (a), and % elongation (b) of glucomannan and glucomannan–xylan biofilms, reinforced with NFC and without NFC, in addition compared with LDPE films (b)

3.3.3 PPS roughness

The PPS roughness was measured (soft backing and a clamping pressure of 1000 Pa). The results (Figure 7) confirmed that the presence of NFC generated more rough surfaces for all biofilms; Gluc90 without NFC displayed the highest roughness of all, 5.94 µm, and the smoothest biofilm was Gluc70 with NFC, 1.36 µm, though it still has higher roughness than LDPE, 0.1 µm.

3.3.4 PPS porosity

The porosity of reinforced Gluc60 has the least value, 0.08 ml/min followed by LDPE film, 0.1 ml/min. The presence of NFC affected the PPS porosity in a good way by making non-porous biofilms, but not in the case of reinforced Gluc50 and Gluc40, maybe because the amount of xylan was increased. Gluc90 without NFC is the most porous biofilm. Figure 7 shows how the NFC helped in blocking the passages for air to flow through the biofilms.

3.3.5 Air permeability

The calculations of air permeability coefficient according to Equation 2 are listed in Table 4 and plotted in Figure 7. The less permeable biofilms were Gluc60, Gluc70, Gluc80 and Gluc40. Gluc50 reinforced with NFC had the maximum air permeability coefficient, 1.3×10^{-6} mm^2 compared to Gluc50 without NFC, while Gluc90 showed the opposite. For LDPE film, the air permeability coefficient was the least value 8.8×10^{-8} mm^2, making it a good barrier of air and other gases, so does Gluc60 and Gluc70.

3.4 Destructive tests

Tensile test and % elongation test for each sample is presented in Figure 8, the latter compared with plastic film LDPE. The plastic film LDPE has the tensile strength of 600 kPa. The reason of this value is the crystallinity of LDPE and long branches that give it strong structure (Bastarrachea, Dhawan and Sablani, 2011). The biofilm of pure glucomannan showed the highest tensile value of all biofilms. From the Figure 8a, we notice that there is a drop of the tensile values as the concentration of the glucomannan is lowered; Gluc100 with NFC had 20 kPa whereas Gluc40 with NFC had 2 kPa. In the other set, non-NFC biofilms, Gluc100 had 16.7 kPa and Gluc40 0.9 kPa. All biofilms with NFC showed a higher value than non-NFC biofilms. It may be explained as glucomannan has the larger polymer chain among other polymers of the biofilm matrix (xylan, NFC and sorbitol) and the bonds between the chains made it stronger.

Similarly, in Figure 8b, the % elongation of the test samples are plotted. The plastic film LDPE elongated 20.6 %, which is more than other samples, and the least was Gluc40 without NFC by only 8 %. The same reasons as in the case of tensile strength can explain the high value of % elongation of LDPE, its crystallinity and branching.

4. Conclusions

Glucomannan or xylan stand-alone biofilms suffered from mechanical and moisture barrier problems. Therefore, in order to solve these problems, composite biofilms with each other and NFC were prepared. In general, we found that adding xylan to glucomannan improved the wettability, reduced the viscosity and lowered the gelation point of the filmogenic solutions compared to pure glucomannan; from film forming aspects, xylan reduced the PPS porosity, air permeability as well as transmittance, tensile strength and elongation. NFC addition to the glucomannan–xylan matrix hindered the gelation point of the filmogenic solutions and improved tensile and elongation at break of the biofilms.

References

Al Ajlouni, K., Fleming P.D. and Pekarovicova, A., 2021. Glucomannan for food packaging biofilms: faceting of the polymer film. In: C. Ridgway, ed. *Advances in Printing and Media Technology: Proceedings of the 47th International Research Conference of iarigai.* Athens, Greece, 19–23 September 2021. Darmstadt: iarigai, pp. 97–109. http://doi.org/10.14622/Advances_47_2021.

Bastarrachea, L., Dhawan, S. and Sablani, S.S., 2011. Engineering properties of polymeric-based antimicrobial films for food packaging. *Food Engineering Reviews*, 3(2), pp. 79–93. https://doi.org/10.1007/s12393-011-9034-8.

Chakravartula, S.S.N., Soccio, M., Lotti, N., Balestra, F., Dalla Rosa, M. and Siracusa, V., 2019. Characterization of composite edible films based on pectin/alginate/whey protein concentrate. *Materials*, 12(15): 2454. https://doi.org/10.3390/ma12152454.

Chen, G.-G., Qi, X.-M., Guan, Y., Peng, F., Yao, C.-L. and Sun, R.-C., 2016. High strength hemicellulose-based nanocomposite film for food packaging applications. *ACS Sustainable Chemistry & Engineering*, 4(4), pp. 1985–1993. https://doi.org/10.1021/acssuschemeng.5b01252.

Deshavath, N.N., Veeranki, V.D. and Goud, V. V., 2019. Lignocellulosic feedstocks for the production of bioethanol: availability, structure, and composition. In: M. Rai and A.P. Ingle, eds. *Sustainable bioenergy: advances and impacts.* Amsterdam: Elsevier. Ch. 1. https://doi.org/10.1016/B978-0-12-817654-2.00001-0.

Grand View Research, 2020. *Food packaging market size, share & trends analysis report, 2020–2027*. [online] Available at: <https://www.grandviewresearch.com/industry-analysis/food-packaging-market> [Accessed 21 Novemer 2021].

Hartman, J., 2006. *Hemicellulose as barrier material*. Licentiate thesis. Kungliga Tekniska Högskolan, Stockholm.

Honarvar, Z., Hadian, Z. and Mashayekh, M., 2016. Nanocomposites in food packaging applications and their risk assessment for health. *Electronic Physician*, 8(6), pp. 2531–2538. https://doi.org/10.19082/2531.

Hu, L., Du, M. and Zhang, J., 2018. Hemicellulose-based hydrogels present status and application prospects: a brief review. *Open Journal of Forestry*, 08(1), pp. 15–28. https://doi.org/10.4236/ojf.2018.81002.

Ingle, J.D. and Crouch, S.R., 1988. *Spectrochemical analysis*. Englewood Cliffs, NJ: Prentice Hall.

International Organization for Standardization, 2019. *ISO 13468-1:2019 Plastics – Determination of the total luminous transmittance of transparent materials – Part 1: Single-beam instrument*. Geneva: ISO.

IGT team, 2021. *IGT Testing Systems: surface characteristics.* [online] Available at: <https://www.igt.nl/laboratory-testing/surface-characteristics/> [Accessed 9 November 2021].

Kalia, S., Dufresne, A., Cherian, B.M., Kaith, B.S., Avérous, L., Njuguna, J. and Nassiopolous, E., 2011. Cellulose-based bio- and nanocomposites: a review. *International Journal of Polymer Science*, 2011: 837875. https://doi.org/10.1155/2011/837875.

Kunlere, I.O., Fagade, O.E. and Nwadike, B.I., 2019. Biodegradation of low density polyethylene (LDPE) by certain indigenous bacteria and fungi. *International Journal of Environmental Studies*, 76(3), pp. 428–440. https://doi.org/10.1080/00207233.2019.1579586.

Lopez, C.G. and Richtering, W., 2021. Oscillatory rheology of carboxymethyl cellulose gels: influence of concentration and pH. *Carbohydrate Polymers*, 267: 118117. https://doi.org/10.1016/j.carbpol.2021.118117.

Ma, R., Pekarovicova, A. and Fleming, P. D., 2018. Biopolymer films from glucomannan: the effects of citric acid crosslinking on barrier properties. *Journal of Print and Media Technology Research*, 7(1), pp. 19–25. https://doi.org/10.14622/JPMTR-1802.

Makkonen, L., 2016. Young's equation revisited. *Journal of Physics: Condensed Matter*, 28(13): 135001. https://doi.org/10.1088/0953-8984/28/13/135001.

Morrison, F.A., 2001, *Understanding rheology.* Oxford, New York: Oxford University Press.

Nechita, P. and Roman, M., 2020. Review on polysaccharides used in coatings for food packaging papers. *Coatings*, 10(6): 566. https://doi.org/10.3390/COATINGS10060566.

Now Foods, n.d. Now foods, glucomannan, pure powder, 8 oz (227 g). *Foodpharmacy Blog*, [blog]. Available at: <https://foodpharmacy.blog/now-foods-glucomannan-2.html> [Accessed 21 November 2021].

Pal, L., Joyce, M.K. and Fleming, P.D., 2006. A simple method for calculation of the permeability coefficient of porous media. *Tappi Journal*, 5(9), pp. 10–16.

Picout, D.R. and Ross-Murphy, S.B., 2003. Rheology of biopolymer solutions and gels. *The Scientific World Journal*, 3: 524215, pp. 105–121. https://doi.org/10.1100/tsw.2003.15.

Sasmitaloka, K.S., Arif, A.B., Juniawati, Winarti, C., Hayuningtyas, M., Ratnaningsih and Richana, N., 2019. Xylan production from corn cobs for osolation of xylanase-producing bacteria. In: *IOP Conference Series: Earth and Environmental Science, 309: 2nd ICAPHP.* Kuta, Bali, Indonesia, 29–31 August 2018. IOP Science. https://doi.org/10.1088/1755-1315/309/1/012066.

Scheller, H.V. and Ulvskov, P., 2010. Hemicelluloses. *Annual Review of Plant Biology*, 61(1), pp. 263–289. https://doi.org/10.1146/annurev-arplant-042809-112315.

Shi, X.-D., Yin, J.-Y., Cui, S.W., Wang, Q. and Nie, S.-P., 2020. Plant-derived glucomannans: sources, preparation methods, structural features, and biological properties', *Trends in Food Science & Technology*, 99, pp. 101–116. https://doi.org/10.1016/j.tifs.2020.02.016.

Technical Association of the Pulp and Paper Industry, 2010. *TAPPI T 555 Roughness of paper and paperboard (Print-surf method)*. Peachtree Corners, GA: TAPPI.

Triantafillopoulos, N., 1988. *Measurement of fluid rheology and interpretation of rheograms*. 2nd ed. Novi, Michigan: Kaltec Scientific.

Wang, K., Wu, K., Xiao, M., Kuang, Y., Corke, H., Ni, X. and Jiang, F., 2017. Structural characterization and properties of konjac glucomannan and zein blend films. *International Journal of Biological Macromolecules*, 105, pp. 1096–1104. https://doi.org/10.1016/j.ijbiomac.2017.07.127.

Wu, C., Li, Y., Du, Y., Wang, L., Tong, C., Hu, Y., Pang, J. and Yan, Z., 2019. Preparation and characterization of konjac glucomannan-based bionanocomposite film for active food packaging. *Food Hydrocolloids*, 89, pp. 682–690. https://doi.org/10.1016/j.foodhyd.2018.11.001.

Yoshimura, M., Takaya, T. and Nishinari, K., 1998. Rheological studies on mixtures of corn starch and konjac-glucomannan. *Carbohydrate Polymers*, 35(1–2), pp. 71–79. https://doi.org/10.1016/S0144-8617(97)00232-4.

Zhong, L.-X., Peng, X.-W., Yang, D., Cao, X.-F. and Sun, R.-C. 2013. Long-chain anhydride modification: a new strategy for preparing xylan films. *Journal of Agricultural and Food Chemistry*, 61(3), pp. 655–661. https://doi.org/10.1021/jf304818f.

Appendix: Frequency sweep for glucomannan–xylan filmogenic solutions

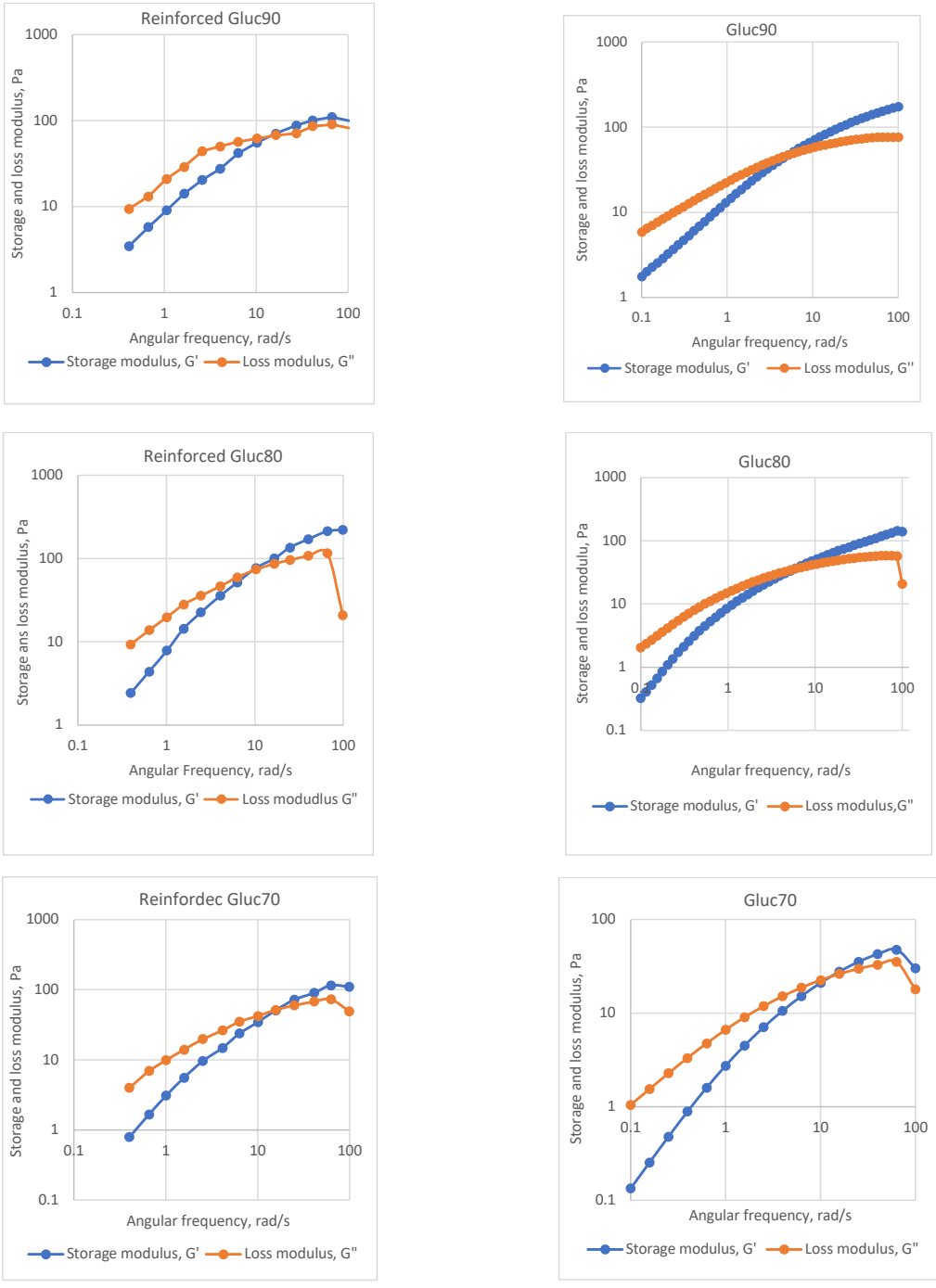

a) *b)*

Figure A1: Frequency sweep for glucomannan–xylan filmogenic solutions, reinforced with NFC (a) and without NFC (b) – part 1

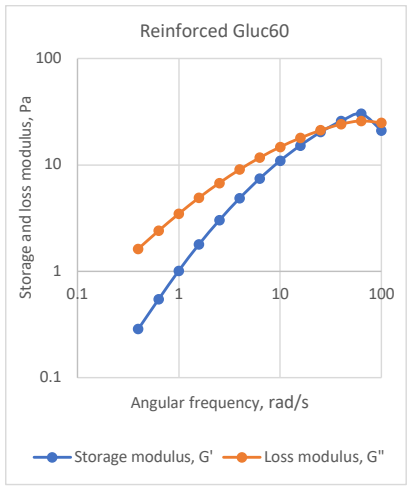

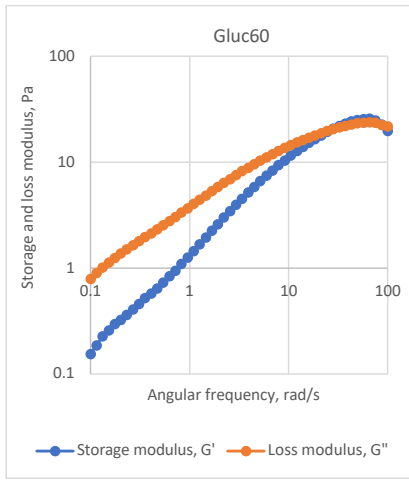

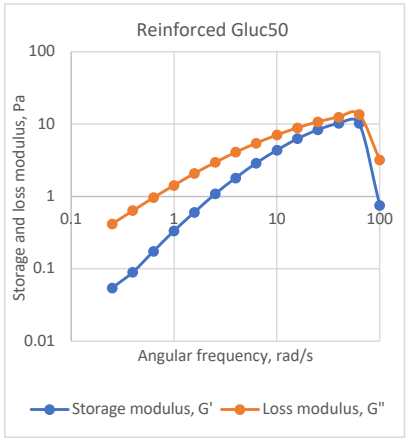

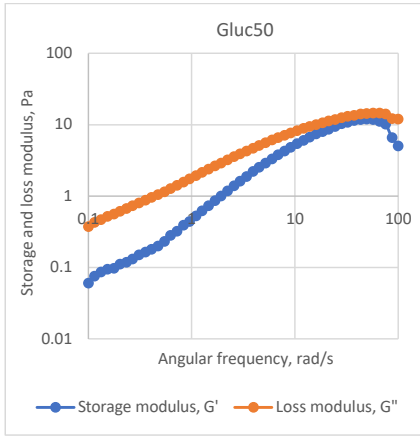

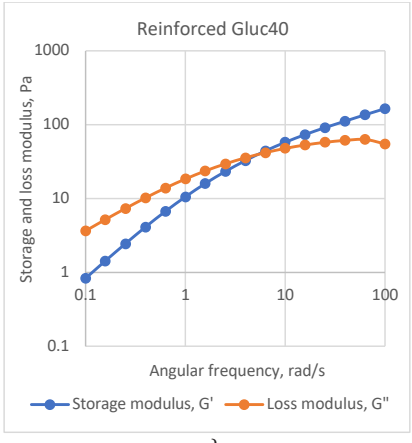

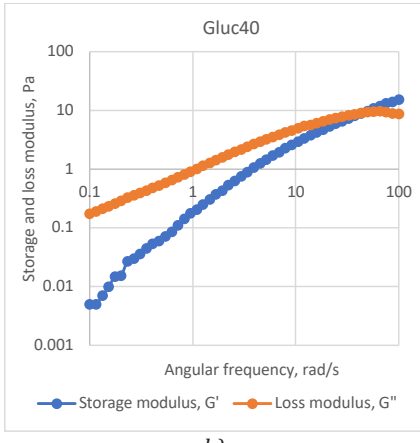

a) *b)*

Figure A1: Frequency sweep for glucomannan–xylan filmogenic solutions, reinforced with NFC (a) and without NFC (b) – continued